Beam Dynamics Studies for a Laser Acceleration Experiment[*]

E. Colby, R. Noble, D. Palmer, R. Siemann and J. Spencer[†]
SLAC, Menlo Park, CA 94025, USA

Abstract

The NLC Test Accelerator (NLCTA) at SLAC was built to address various beam dynamics issues for the Next Linear Collider. An S-Band RF gun is being installed together with a large-angle extraction line at 60 MeV followed by a matching section, buncher and final focus for the laser acceleration experiment, E163. The laser-electron interaction area is followed by a broad range, high resolution spectrometer (HES) for electron bunch analysis. Another spectrometer at 6 MeV will be used for analysis of bunch charges up to 1 nC. Emittance compensating solenoids and the low energy spectrometer (LES) will be used to tune for best operating point and match to the linac. Optical symmetries in the design of the 25.5° extraction line provide 1:1 phase space transfer without use of sextupoles for a large, 6D phase space volume and range of input conditions. Design techniques, tolerances, tuning sensitivities and orthogonal knobs are discussed.

INTRODUCTION

Because the NLCTA[1] is an existing facility, a number of constraints had to be accommodated for the experiment. While E163 needs only low emittance, 50 pC bunches, the NLCTA requires a variety of bunch characteristics with charges up to 1 nC. The thermionic gun is being replaced by an S-band RF gun similar to one originally proposed for the NLCTA and the ORION facility[2]. Beyond the usual gun and cathode diagnostics, a low energy spectrometer (LES) will allow analysis of ≤7 MeV beams with good resolution within the 1.5 m transport line between cathode and X-band linac.

For E163, a new beam line will exit the NLCTA at 60 MeV after 2, 0.9 m linac sections and a chicane followed by a 4-quad matching section. At this point, a large, exit-angle bend of 25.5° from the NLCTA will provide beam to a new experimental area[2] through a 6 foot concrete shield wall. To minimize η and η' outside as well as η in the quads used for this, a symmetric, two-bend dogleg with two quad triplets enclosed allows a nearly perfect match to the linac that is then relayed to the laser-electron interaction region via a doublet for matching and a final focus triplet. The interaction region is followed by another, high energy spectrometer (HES) which analyzes the resulting electron bunches with high resolution. Figure 1 shows the design layout which is discussed with emphasis on beam dynamics, optical transport, optimization and analysis systems.

REQUIREMENTS AND DESIGN

A summary of the experimental requirements for E163 is given in Table 1. The more demanding of these are the energy spread and timing jitter from the small electron energy modulation signal expected[3] from the laser interaction and the need for the electron and laser beams to arrive at the same location within the laser pulse. To keep the rf induced energy spread low in the NLCTA linac requires short electron bunches of order 0.1 mm (0.4 psec). Obtaining short bunches from an rf gun is straightforward at the reduced charge for E163 (50 pC) where transverse emittances are not too demanding[3]. Beam dynamics studies have been separated into those required to understand the production of low energy-spread beams out of the NLCTA linac and those to demonstrate the transport and matching of these beams to the experiment for a range of currents.

BEAM DYNAMICS STUDIES

Detailed simulations of the beam dynamics for the NLCTA with the rf gun included have been completed through the NLCTA and E163 beamlines using the computer codes Parmela[4], Transport[5] and Elegant[6]. These beamlines pose several challenges: injection from an S-band gun into an X-band accelerator requires the production of higher density bunches than is typically optimal to suppress rf-induced emittance growth in the accelerator; the present NLCTA chicane is a 3π phase advance design permitting wide variation of the temporal dispersion (R56), but at the expense of strong second-order aberrations in the horizontal plane; the beamline leading to the hall is connected via a 25.5° dogleg with strong space constraints while requiring careful matching and second-order temporal and spatial dispersion (T566,T166 etc.) control to preserve the phase space of potential, higher charge bunches.

The various codes were used to complement one another for space charge, synchrotron radiation and higher order optical effects. For the latter, we normalized the 6D phase space variables to a unit hypersphere enclosing most phase space volumes expected for 1 nC bunches.
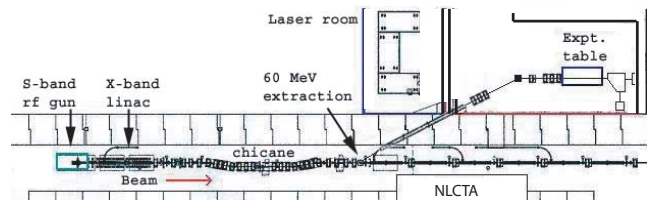

Figure 1: Schematic layout of the NLCTA and E163 lines.

The Photoinjector System

The E163 photoinjector line is designed to permit both high charge (1 nC) operation for NLCTA tests and the low charge (50 pC) operation for laser acceleration experiments. The injection line length (150 cm) and solenoid (3 kG, 25 cm length) were designed to enable transverse emittance compensation for high charge operation, as is standard in high-brightness photoinjectors. For laser acceleration, accelerator parameters are adjusted instead to achieve low energy spread. The solenoid is tuned to provide a mildly converging beam approaching a waist (<1 mm rms) near the x-band linac entrance. The bunch starts out 5 mm wide by 0.1 mm long to keep its charge density low in the gun and reduce rf-induced energy spread in the linac. The gun operates at a nominal 105 MV/m surface field and 30 degrees phase after rf crossing to maintain the bunching. In the drift between the gun and linac, the 4-6 MeV bunch naturally develops a correlated energy spread (1 %) due to space charge. The beam is accelerated 5-10° before the crest in the x-band linacs to counteract this correlated energy spread to about 0.05 % at 60 MeV as needed by the experiment for ≤50 pC bunches.

Table 1: Characteristics and Parameters for E163

Beam Energy E [MeV]	6 at Source; 60 at Expt.
Rep. Rate $f_{\rm rep}$[Hz]	10
Bunch Charge N_B[nC]	$0.01 - 1.0$
Emittance ϵ_{xN}; ϵ_{yN} [10^{-6}m]	≤ 2.5 ; ≤ 2.5
Energy Spread $\delta E_{rms}/\bar{E}$[%]	< 0.065
RMS Bunch Length[ps]	0.4(0.05 nC)
	1.8(0.25 nC)
Charge Stability	± 2.5 % pulse-to-pulse
RMS Timing Jitter [ps]	0.25
LES Resolving Power	4000
HES Resolving Power	10000
Photoinjector	1.6 Cell, S-band
Drive Laser	Ti:Sap(266nm,0.15 mJ)
Source RF System	SLAC 5045 Klystron
S-band(2.856 GHz)	Solid State Modulator
Injector Linac	Two 0.9 m sections
X-band(11.424 GHz)	30 MV/m structures

The Low Energy Spectrometer (LES) A stronger solenoid strength allows a foreshortened waist at the nominal object of the LES located about midway between the cathode and the linac. For an object at 27.6 cm from the bend pivot, the image has good depth of field around 40 cm from the pivot for a 1.25 rad vertical bend having shim angles at entrance and exit of 0.50,0.0 rad. Defining the lowest-order resolving power as:

$$RP_1 \equiv \frac{\eta_y}{\sqrt{\beta_y \epsilon_y}} = 1.4\,\eta{\rm [mm]}\Big[\frac{E{\rm [MeV]}}{\beta{\rm [m]}\epsilon_n{\rm [\mu m]}}\Big]^{\frac{1}{2}} \quad (1)$$

gives $RP_1 \geq 4000$ for a focused, 50 pC, round bunch with $\{\sigma_{x,x'}, \sigma_{y,y'}, \sigma_z, \delta\} \equiv \{0.0385, 3.55, 0.0385, 3.55, 0.1, 0.8\}$

in units of mm, mr and %. A pixel equal to the monochromatic spot (σ_0=100 μm) with dispersion η=420 mm implies 1.2 keV/px at 5 MeV and acceptance of 0.1 %/mm.

To consider space charge, the plasma wavelength is:

$$\lambda_p{\rm [m]} = \frac{3.3 \cdot 10^4}{\sqrt{{\rm n[cm^{-3}]}}} = 1.50\sqrt{\frac{\gamma\sigma_{\rm x}\sigma_{\rm y}\sigma_{\rm z}{\rm [cm^3]}}{N_B{\rm [nC]}}} \ . \quad (2)$$

Assuming 1 nC for a unit hypersphere (units of mm, mr and %), gives 0.16 m while 50 pC gives 0.73 m. Comparing to an object-to-image distance of less than 0.75 m implies we can't ignore space charge for short bunches in the LES.

Figure 2 shows results for the 50 pC, short-bunch (λ_p=9 mm), with and without space charge, for a symmetric waist at z=0. This shows serious space charge blowup in all dimensions with the energy spread increasing 75 % until the dispersion in the spectrometer stops it - after which it remains constant. For the beam matched into the linac with 50 pC, λ_p=0.37 m with a 33 % increase in energy spread. This demonstrates the space charge problem and is one reason for using the unit hypersphere for design without space charge. Finally, reducing the charge N_B to 5 pC is still worse than the 50 pC case matched to the linac. While space charge significantly increases all normalized emittances in all cases, σ_y and σ_y^{sc}, after the spectrometer, scale as δ_s, the energy spread at the spectrometer's entrance EFB.
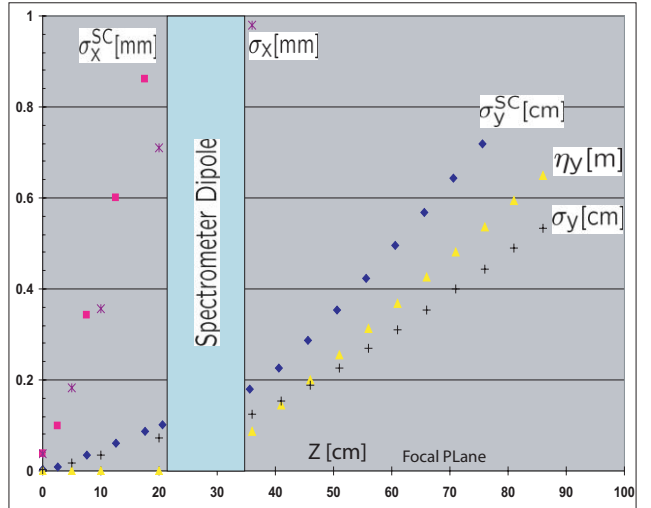

Figure 2: Analysis of space charge(sc) on and off for 50 pC.

Synchrotron radiation also increases the emittance but with a different dependence on beam and Twiss parameters[7]. We estimate this as:

$$\frac{d\epsilon_y}{ds} \approx \frac{2}{3}r_e\frac{\hbar c}{mc^2}F(N_B, \lambda_c, \sigma_z)\frac{\gamma^5}{\rho^3}\frac{\eta^2}{\beta} \ . \quad (3)$$

s is the distance along the bend path of radius ρ and η and β are the local dispersion and betatron functions in the spectrometer. The first terms relate to the synchrotron radiation, F to coherence effects (λ_c is critical wavelength) and the last term to optical effects. Low bend fields with high β's improve RP_1 and balance the large η's that are also needed.

Clearly, $F(N_B, \lambda_c, \sigma_z)$ is the important quantity for such low energies because at 500 μm, $\lambda_c > \sigma_z$. Taking F as proportional to $10(N_B/e)$ implies we can ignore this effect when studying the gun's characteristics as well as at 60 MeV except for extremely high-charge, short bunches.

The E163 Line

The E163 line begins at the image of a quadruplet of quads used for matching out of the chicane as shown in Fig. 1. The bunch then enters the first $25.5°$ dogleg bend that uses both entrance and exit shim angles to minimize dispersion going into the first triplet of quads which is placed as close as possible to the bend. We used an unnormalized, unit hypersphere at 60 MeV for design purposes but with δ=10% in some cases. Our goal was to transport any beam (the hypersphere) from the chicane exit out of the NLCTA with minimal phase space distortion and without using sextupoles since the drift length to the wall was very short and the available space highly constrained.

In the E163 enclosure, the remaining line is very much like LEAP[3] and the spectrometer, a $90°$ sector magnet, will be the same except modified for higher energies.

There are a total of 4 matching quads and 12 – E163 quads in use for the optics and tuning. Each of these have two trim windings that can be wired as either dipole or quadrupole and, in most cases, an independent primary current that can be used for tuning. The dogleg triplets are matched sets run in series, as are the dogleg bends, to emphasize symmetry about the midpoint of this section to help minimize dispersion throughout the system and give $\eta = \eta' = 0$ at the exit before a matching doublet.

Tuning the system is done between match points into the first linac section, after the second, in front of the chicane, and in front of the first dogleg bend in the NLCTA. The 50 pC, 60 MeV bunch out of the linac and before the chicane is round with σ_r=0.8 mm, $\sigma_{r'}$=0.02 mr, σ_z=0.16 mm and δ=0.05 % which gives λ_p=0.75 m. Sensitivity to changes in control parameters here are given in Table II. The bunch length, set by the laser, is σ_t=0.4 ps ($1.68°$ X-band), truncated at $\pm 2\sigma_t$. The rf gun phase is $30°$ (S) after zero-crossing to provide strong bunching and the nominal gradient is G_G=42.6 MV/m (surface field 105 MV/m). Transverse emittance is less important so the initial size is σ_r=0.25 cm to reduce space-charge effects due to the short bunch. Space charge still increases the energy spread to $\approx 0.8\%$ as the 5 MeV beam drifts between gun and linac. The phases in the two linac sections are set to 81 and 86 degrees (X), after zero crossing, so that electron acceleration occurs ahead of the crest, resulting in a reduction of energy spread during acceleration to 60 MeV. Linac gradients are G_l=30 MV/m to reduce breakdown. Solenoid focusing (B=0.2 T) is adjusted for convergence into the linac (σ_r=0.9 mm, β=4.38 m, α= 3), while adjusting linac phases to minimize energy spread at 60 MeV (σ_E=0.05%) at the expense of transverse emittance (ϵ_n=2 μm).

Table 2: Initial sensitivity studies for Experiment E163

Derivative-Dimensionless	Sensitivity*
$\delta\sigma_r/\delta B \cdot (B/\sigma_r)$	$-4_1, -12_2, -25_i, -12_o$
$\delta\epsilon_n/\delta B \cdot (B/\epsilon_n)$	-7 B(↕)
$\delta\sigma_{E_o}/\delta B \cdot (B/\sigma_{E_o})$	13 for B(↑)
$\delta\sigma_{E_o}/\delta\sigma_r^L \cdot (\sigma_r^L/\sigma_{E_o})$	-1 for σ_r^L (↓)
$\delta\sigma_{E_o}/\delta\sigma_t^L \cdot (\sigma_t^L/\sigma_{E_o})$	1 for σ_t^L (↑)
$\delta\sigma_{E_o}/\delta N_B \cdot (N_B/\sigma_{E_o})$	2 for N_B (↑)
$\delta E_o/\delta\phi_G/E_o$	.15%/1°S(↑);-.35%/1°S(↓)
$\delta E_{o}/|\delta\phi_G| \cdot (\phi_G/\sigma_{E_o})$	57
$\delta\phi/\delta\phi_G$ (linac arrival ϕ)	$3°$(X)/$1°$(S)
$\delta E_o/\delta G_G \cdot (G_G/E_o)$	0.017 ($G_G\equiv$Gun gradient)
$\delta\sigma_{E_o}/|\delta G_G| \cdot (G_G/\sigma_{E_o})$	180
$\delta E_o/\delta G_l \cdot (G_l/E_o)$	0.45 ($G_l\equiv$linac gradient)

*Values are at linac exit (o) – otherwise at screen 1, 2 or linac entrance i. Derivatives are for increasing $\equiv$(↑), decreasing $\equiv$(↓) or symmetric $\equiv$(↕). No direction arrow implies insensitivity to that direction or symmetric.

For the remaining sections, matching quads can be used to set the beam up for best transfer through the dogleg or tuning of different configurations to the next match point or tune for small spots at the laser IP. The latter case is useful because it helps to remove possible errors throughout the complete transport line. If we change the i-th quad strength by δk, the output matrix changes by:

$$\frac{\delta m_{11}}{\delta k} = -m_{12} \quad \text{and} \quad \frac{\delta m_{21}}{\delta k} = -m_{22} . \tag{4}$$

One can then check which quads are most effective and independent in both planes for any function or location. Because many quads are used for steering this is a good global correction for unavoidable hysteresis but requires good knowledge of the input Twiss parameters e.g. to minimize β_o and α_o at some output location:

$$\beta_o = \frac{m_{12}^2}{\beta_i} \quad \text{and} \quad \alpha_o = -\frac{m_{22}}{m_{12}}\beta_o . \tag{5}$$

ACKNOWLEDGMENTS

REFERENCES

[1] R. Ruth, et al., "The Next Linear Collider Test Accelerator", PAC1993, Washington, D.C., May 1993. For complete report: SLAC-PUB-6293, July 1993.

[2] R. Noble, et al., "The Orion Facility", PAC2003, Portland, OR, May 2003.

[3] T. Plettner, et al., "The LEAP Experiment at Stanford", PAC1999, New York, NY, May 1999.

[4] H. S. Deavon, et al., LA-UR-90-1766, p. 137 (1990).

[5] D.C. Carey, et al., "Third-Order Transport", SLAC-R-95-462, May 1995

[6] M. Borland, "Elegant", APS LS-287, Sept. (2000) and M. Borland et al., PAC2003, Portland, OR, May 2003.

[7] A. Chao and M. Tigner, Ed's., "Handbook of Accelerator Physics", World Publishing, Singapore, 2002.